Clim. Past, 7, 437–450, 2011
www.clim-past.net/7/437/2011/
doi:10.5194/cp-7-437-2011


Climate of the Past

# Links between MIS 11 millennial to sub-millennial climate variability and long term trends as revealed by new high resolution EPICA Dome C deuterium data – A comparison with the Holocene

**K. Pol[1], M. Debret[2], V. Masson-Delmotte[1], E. Capron[1], O. Cattani[1], G. Dreyfus[1,3], S. Falourd[1], S. Johnsen[4], J. Jouzel[1], A. Landais[1], B. Minster[1], and B. Stenni[5]**

[1]Laboratoire des Sciences du Climat et de l'Environnement, IPSL, CEA CNRS UVSQ, UMR 8212, CEA Saclay, L'Orme-des-Merisiers, 91191 Gif-Sur-Yvette Cedex, France
[2]Laboratoire De Morphodynamique Continentale et Côtière – UMR CNRS 6143, Bât IRESE A, Département de Géologie, Université de Rouen, 76821 Mont Saint Aignan Cedex, France
[3]Department of Geosciences, Princeton University, Princeton, NJ, USA
[4]Centre for Ice and Climate, Niels Bohr Institute, University of Copenhagen, Juliane Maries Vej 30, 2100 Copenhagen, Denmark
[5]Università di Trieste, Dipartimento di Scienze Geologiche, Ambientali e Marine, Via E. Weiss 2, 34127 Trieste, Italy

Received: 28 July 2010 – Published in Clim. Past Discuss.: 20 September 2010
Revised: 2 March 2011 – Accepted: 11 March 2011 – Published: 29 April 2011

**Abstract.** We expand here the description of the Antarctic temperature variability during the long interglacial period occurring ∼400 thousand years before the present (Marine Isotopic Stage, MIS 11). Our study is based on new detailed deuterium measurements conducted on the EPICA Dome C ice core, Antarctica, with a ∼50 year temporal resolution. Despite an ice diffusion of a length reaching ∼8 cm at MIS 11 depth, the data allow us to highlight a variability at multi-centennial scale for MIS 11, as it has already been observed for the Holocene period (MIS 1). The differences between MIS 1 and MIS 11 are analysed regarding the links between multi-millennial trends and sub-millennial variability. The EPICA Dome C deuterium record shows an increased variability and the onset of millennial to sub-millennial periodicities at the beginning of the final cooling phase of MIS 11. Our findings are robust with respect to sensitivity tests on the somewhat uncertain MIS 11 duration.

*Correspondence to:* K. Pol
(katy.pol@lsce.ipsl.fr)

## 1 Introduction

Past interglacials, free from human impact on climate, are nowadays well documented by climatic records long available, such as marine sediment (Lisiecki and Raymo, 2005) or ice cores (Jouzel et al., 2007; Loulergue et al., 2008; Spahni et al., 2005; Lüthi et al., 2008; Siegenthaler et al., 2005) and offer the possibility to study natural climate variability during warm periods (Tzedakis et al., 2009). Increasing our knowledge of their dynamics is expected to provide a better understanding of the past and future evolution of our present warm climatic period: the Holocene, whose natural course is disturbed by anthropogenic forcings (IPCC, 2007). In this context, the challenge lies in finding the most appropriate past interglacial for a comparison with the Holocene period. Occurring in an orbital configuration close to the recent one (low eccentricity) around 400 thousand years before the present day (kyr BP, hereafter noted ka), Marine Isotopic Stage (MIS) 11 was proposed to be a good candidate, according to a high correlation between the mean 65° N June insolations of MIS 1 (or Holocene) and 11 (Loutre and Berger, 2000, 2003). Although the Antarctic temperature derived from the EPICA Dome C (EDC) isotopic data (Jouzel et al., 2007) exhibits values up to +2 °C higher than the mean value for present day at MIS 11 maximum (dated around

Published by Copernicus Publications on behalf of the European Geosciences Union.

406 ka using the EDC3 chronology, Parrenin et al., 2007), $CO_2$ (Siegenthaler et al., 2005) and $CH_4$ (Spahni et al., 2005) concentrations reach similar levels, around 280 ppm and 710 ppb respectively, during MIS 11 and the preindustrial period. Moreover, recent sea-level records (Bowen, 2010; Rohling et al., 2010) converge towards an estimation of sea-level at ∼400 ka, comparable with the present one as it was previously suggested by McManus et al. (2003) and Waelbroeck et al. (2002) and modelled by Bintanja et al. (2005).

The climatic contexts of MIS 1 and 11 thus present interesting similarities. Controversies have however emerged regarding the orbital alignment of the two interglacials with implications for the prediction of the MIS 1 duration. The debate summarized in Tzedakis (2010) arises from the choice of aligning either precession (Loutre and Berger, 2000, 2003; Ruddimann, 2005, 2007) or obliquity (EPICA-community-members, 2004; Masson-Delmotte et al., 2006) for the synchronisation of the two interglacials. A recent marine study (Dickson et al., 2008) tends to support the alignment of obliquity. Nevertheless, the double-peak precession configuration of MIS 11 still contrasts with the orbital context of MIS 1, which is marked by a single precession maximum. A careful comparison with earlier past interglacials now appoints MIS 19 as the warm climatic period with the closest orbital configuration to the Holocene one (Pol et al., 2010; Rohling et al., 2010; Tzedakis, 2010). The study of MIS 19, remains, however, difficult due to age-scale uncertainties as well as the lack of high-resolution records (Pol et al., 2010). Instead, MIS 11 offers the ability to document natural climate variability along the longest interglacial recorded since one million years ago and the establishment of the 100 kyr glacial-interglacial cycles (Bintanja et al., 2005; Jouzel et al., 2007; Lisiecki and Raymo, 2005) at high resolution.

While earlier comparisons of MIS 11 and Holocene focused on the analysis of their trends or amplitudes (EPICA-community-members, 2004; Masson-Delmotte et al., 2006), we propose here to analyse the Antarctic high frequency climate variability within these two periods. Our study relies on new high-resolution measurements of water stable isotope ratios (deuterium/hydrogen ratio expressed as $\delta$D) conducted on the EDC ice core, which have improved the temporal resolution for MIS 11 (Sect. 2). This new resolution, close to the Holocene one (∼20 years), allows us to better document and compare MIS 1 and 11 Antarctic temperature fluctuations at sub-millennial scale in two different ways: (i) by studying the $\delta D$ record variance changes in relationship with long term trends, which was not possible with the previous MIS 11 $\delta D$ bag data because of the lack of a sufficient number of points; (ii) by performing spectral analyses of our $\delta D$ signals. Section 3 is dedicated to the description of the methods before the results are presented in Section 4 and the variability analyses (Sect. 5) in detail. Spectral analyses are highly dependent on the age-scale and on the estimation of MIS 11 duration. As differences have been reported between the EDC3 chronology (Parrenin et al., 2007) used in Jouzel et al. (2007) and other age-scales (Kawamura et al., 2010; Lisiecki and Raymo, 2005), we performed sensitivity tests for different MIS 11 durations, compatible with orbital constrains derived from available and new EDC air data records, and discuss the robustness of our variability analyses. And finally, we investigated the possible mechanisms at the origin of the observed $\delta D$ variability during MIS 1 and 11 periods (Sect. 6).

## 2 Material

The EDC site in East Antarctica (75°06′ S, 123°2′ E) has provided ∼3260 m of ice core. Derived from the measurements of 5800 samples coming from the continuous cut every 55 cm of the core ("bag samples"), a first long $\delta D$ record unveiling ∼800 ka of local temperature variations was provided (Jouzel et al., 2007). In central Antarctica, the climatic information imprinted in surface snow stable isotope composition is affected by post deposition processes such as firn diffusion and wind scouring. Detailed signal-to-noise studies conducted at Vostok have shown an effective preservation of the climate signal at a temporal resolution of ∼20 years (Ekaykin et al., 2002). In EDC, the 55 cm sampling allows us to document Holocene climate variability at this temporal step of ∼20 years (Masson-Delmotte et al., 2004). But, due to ice thinning, it describes past interglacials at a lower temporal resolution. A second cut of the EDC core providing 11 cm long samples, called "fine samples" (Pol et al., 2010), increased the depth resolution by a factor of 5, thus improving the temporal resolution for stable isotope records over past interglacials.

Referring to the threshold of $-403‰$ as an arbitrary definition of Antarctic warm periods (related to the lowest 300 year average $\delta D$ value observed over the past ∼12 ka, EPICA-community-members, 2004), the MIS 11 warm Antarctic phase is found in the depth interval from ∼2699 to 2779 m. This interval is dated between ∼395 and 426.7 ka, according to the official time-scale for the EDC core (EDC3 by Parrenin et al., 2007), with an uncertainty of ∼6 kyr on absolute ages and of ± 20% on MIS11 duration (estimated at ∼32 kyr). Here, we have extended the study up to ∼2694 m, thus covering a time interval from ∼392.5 to 426.7 ka, in order to also depict the glacial inception. The MIS 11 temporal resolution available derived from the $\delta D$ bag data (Jouzel et al., 2007) has been contained between 170 and 300 years within the studied interval (the evolution of bag resolution with respect to depth is displayed in Pol et al., 2010). With the new high-resolution $\delta D$ measurements conducted on 770 fine samples, the stable isotope variability is now documented at a resolution ranged between ∼35 and 60 years.

## 3 Methods

### 3.1 Deuterium measurements

The method for deuterium analysis is the same as for the original bag samples measurements. Water is reduced on uranium to form $H_2$ gas as described in Vaughn et al. (1998) for measuring fine samples, including ∼30% replicate measurements. Data are given with an analytical accuracy of $\pm 0.5‰$ at $1\sigma$. The coherency between bag and fine samples during the MIS 11 period can be checked with the calculation of an average signal on 5 fine cut data. The signal derived from the individual bag samples is statically less accurate ($0.5‰$ at $1\sigma$) than the average signal ($\pm 0.23‰$ at $1\sigma$), as it benefits from an experimental noise reduced by a factor of $\sqrt{5}$; this can be explained by the use of 5 measurements for its establishment instead of one for the bag samples profile, over the same 55 cm depth interval.

### 3.2 Correction for isotopic diffusion

Water-stable isotopes undergo firn and ice isotopic diffusion. After snow deposition, such processes gradually smooth isotope profiles by removing the highest frequency climatic information first during firnification (Johnsen, 1977; or more recently Neumann and Waddington, 2004) and then in the solid ice (Ramseier, 1967). In the upper part of the firn, direct exchanges between snow water molecules and vapour involving sublimation-condensation processes erase high frequency isotopic variations. In solid ice, smoothing results from the temperature-dependent molecular diffusivity of water-stable isotopes causing self-diffusion inside ice crystals.

Diffusion models can be applied to a given ice core to evaluate the smoothing of isotope profiles using the diffusion length $\sigma_l$ (characteristic length in cm of an ice layer affected by the smoothing at a given depth), and to reconstruct the original amplitude of climatic variations (back diffused signals). Here we used the Johnsen et al. (2000) method, with the implementation of the parameters suitable for the EDC core (see Pol et al., 2010), on our new $\delta D$ data. A spectral analysis with respect to depth (cycles/m) of the high- resolution signal was performed and the associated red noise of the power spectrum was translated into a diffusion length. This relies on the following equation $A = A_0 \cdot \exp\left(-\frac{1}{2}\sigma_l^2 \cdot k^2\right)$, which links the amplitude of a given harmonic cycle A recorded in the data and altered by the diffusion within the ice, to the initial amplitude $A_0$ (with $\sigma$ the diffusion length and k the wave number associated to the harmonic cycle). The empirical diffusion length at the MIS 11 depth, estimated here to be ∼8 cm according to our high-resolution data, allowed us to reconstruct the original amplitude of climatic variations recorded in the isotopic signal.

We cannot expect to preserve climatic information below ∼20 years in central Antarctica, considering post-depositional processes (Ekaykin et al., 2002), even though the bag samples are supposed to describe the Holocene period at a better temporal resolution (from 8 years at the top of the core to 18 years at ∼12 ka depth). The isotopic diffusion occurring in the upper part of the core only affects the part of the signal that is supposed to highlight periodicities lower than 20 years. Therefore, the isotopic diffusion is considered insignificant for the Holocene record studied here.

### 3.3 Variance analysis

To characterize the new information about MIS 11 climatic variability revealed by the high-resolution EDC $\delta D$ data, we first resample our signals (original and back-diffused ones) on a regular time-step. In the MIS 11 time interval dedicated to the variability study (see Sect. 5), the lowest available temporal resolution is of ∼50 years. The 50 year resampling is thus imposed to avoid extrapolation. For Holocene $\delta D$, we have chosen to keep the 20 year time-step in order to highlight all information than can be accessed at this optimal resolution. The long-term trends, calculated using a Singular Spectrum Analysis (SSA method) and representing multi-millennial scale climatic variations, are then subtracted from the signals to focus on the millennial to sub-millennial scale variability (<5000 years). The variance of the signals is then described using a running standard deviation calculated on the detrended signals, over 3 kyr from the past to the next 1.5 kyr at a given time point. This time period is an arbitrary choice for describing the high frequency variability on a millennial scale; it is constrained by the duration of MIS 1 and the temporal resolution available for MIS 11. Given the normal distribution of deuterium variability, the significance of variance changes can be assessed using a Fischer F-test. Significance thresholds differ for the MIS 1 (149 degrees of freedom over 3 kyr intervals) and MIS 11 (59 degrees of freedom). At the 95% confidence level, ratios of standard deviations are significant when they are larger than 15% (MIS 1) and 22% (MIS 11). The main changes in variance described in Sect. 5.1 can therefore be considered as significant. Other tests have been performed using shorter or longer reference lengths without changing the principal features. In order to compare the variability with the trends, we have calculated coherently with the running standard deviation a running average of the trends over each 3 kyr interval.

### 3.4 Spectral analysis

To examine the frequency distribution of the isotopic record, we also performed spectral analyses of our resampled and detrended original $\delta D$ signals. The same analysis on MIS 11 back-diffused signal will not be discussed as it does not provide any supplementary information on the power spectra. Here we used the wavelet analysis method, which is particularly well adapted to describing non-stationarities or changes in frequency and magnitude (Torrence and Compo,

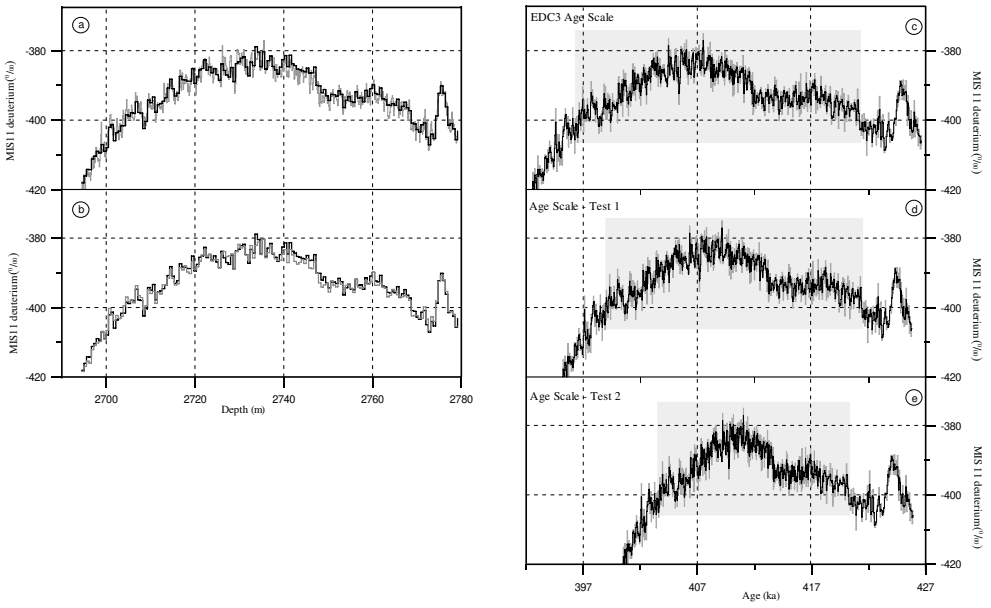


**Fig. 1.** Summary of the available EDC $\delta D$ (‰) data for MIS 11 first plotted for the function of depth (panels a and b, in m) and then for the function of time (panels c to e, in ka). **(a)** $\delta D$ from MIS 11 bag samples (black) and the new high-resolution $\delta D$ signal from the fine samples (grey). **(b)** MIS 11 $\delta D$ bag samples (black) in comparison with the mean signal (grey) obtained from the average of 5 fine cuts. **(c)** High-resolution $\delta D$ data (black) plotted with respect to the official EDC chronology (EDC3, Parrenin et al., 2007) and corrected from the isotopic diffusion (grey). Panels **(d)** and **(e)** display the same signals using two other age-scales (Sect. 5.3) (Test 1 and Test 2 respectively) for sensitivity tests on MIS 11 duration.

1998), common characteristics of climatic records. This method (mathematical formalization described in Mudelsee, 2010) is used to decompose, for different exploratory scales, a signal in a sum of small wave functions of finite length that are highly localized in time, unlike the classical Fourier transform which explores the complete length of the signal and separates it into infinite-length sine-wave functions. Resulting in a loss of time information, the Fourier analysis thus fails to detect the time-variable statistical properties of stochastic processes.

To avoid edge effects and spectral leakage produced by the finite length of the time series, these last ones were zero-padded to twice the data length. Unfortunately, this leads to the underestimation of the lowest frequencies near the edges of the spectrum. It is thus necessary to assess the areas (known as cones of influence) which delineate the parts of the spectrum where estimated energy bands are likely to be less powerful than they actually are. For all local wavelet spectra, Monte Carlo simulations were then used to assess the statistical significance of peaks. The background noise for each signal was first separated and estimated using singular spectrum analysis. Secondly, an autoregressive simulation was performed for each noise time series to determine the AR(1) stochastic process, against which the initial time series had to be tested. The estimated power spectra were tested here against a background red noise (AR(1) = 0.7); the confidence levels were taken above 99%, consistently with the recommended level of 1-1/(1-n) (Thomson, 1990), where n is the number of points in the time interval of interest (580 and 570 for MIS 1 and 11 respectively considering the resampled signals).

## 4 Results

Figure 1 (panel a) displays the results from our new high-resolution $\delta D$ measurements (grey) for MIS 11 depths (from 2694 to 2799 m), confronted to the initial low resolution $\delta D$ signal (black), published in EPICA-community-members (2004) and in Jouzel et al. (2007). It is important to notice here that the new high-resolution data confirm the patterns originally exhibited by the black curve. An abrupt event – also exhibited by the $CO_2$ (Spahni et al., 2005) and $CH_4$ (Loulergue et al., 2008) records – is observable at ∼2775 m. It is followed by a slow warming and then a small decrease between depths of ∼2770 and 2750 m, the maximum of $\delta D$ being reached at ∼2735 m, before the beginning of the cooling phase. The comparison over the same 55 cm depth interval between the "calculated" signal (Fig. 1b, grey) obtained from the average of 5 high-resolution data (see Sect. 3.1) and the previous low resolution profile (Fig. 1b, black) shows a close agreement over the full period, within their respective accuracy (refer to the Sect. 3.1), and confirms the robustness of the measurements. Differences of 1‰ on average and up to 2‰ can be nevertheless observed during the warming phase over depth intervals ranging between 2740 and 2746 m or 2760 and 2766 m. In parallel, the new data

have been used for the calculation of the EDC $\delta D$-excess during MIS 11. The quality of the new high-resolution $\delta D$ measurements is confirmed by stronger correlation with $\delta^{18}O$ bag data (B. Stenni, personal communication, 2010) over the MIS 11 period ($R^2 = 0.98$ using the average of the detailed $\delta D$ data versus 0.97 using the initial bag $\delta D$ data), as well as by the smaller dispersion with respect to this linear regression ($\sim$0.8 versus 1.1‰). This comforts us as to the reliability of our new deuterium measurements.

Thereafter, we focussed on the added information brought in by the high-resolution $\delta D$ data, the signal being examined with respect to time. The reference time-scale for the EDC core is the EDC3 chronology established by Parrenin et al. (2007). Figure 1c displays the high-resolution $\delta D$ signal on the corresponding time interval from $\sim$392 to $\sim$427 ka. The signal corrected for isotopic diffusion is shown in grey and exhibits increased variability up to 2‰.

## 5 Variability analysis: MIS 1 and 11 comparison

Our new $\delta D$ data for MIS 11 now enable a detailed comparison of climate variability below millennial scale during MIS 1 and 11, referring to comparable temporal resolutions of $\sim$50 years and $\sim$20 years respectively. Holocene is scrutinized from the present day to 11.7 ka. (beginning of the plateau just after the Antarctic Cold Reversal, Jouzel et al., 1995, 2001), MIS 11 from 397 to 421 ka (Fig. 1c, grey area), to avoid the difficulty of correctly capturing both the first abrupt event around $\sim$425 ka and the abrupt cooling after 397 ka using the SSA method. Panels a of Fig. 2 display the resampled $\delta D$ signals (initial ones in black and MIS 11 back diffused one in grey) and the calculated trends (red) over the two interglacials. The signals are centred on their respective mean value, $\sim -396$‰ for Holocene and $\sim -391$‰ for MIS 11, with a $\delta D$ difference of 5‰ corresponding to a $\sim$0.8 °C temperature gradient according to the modern spatial slope of 6‰ per °C (Masson-Delmotte et al., 2008) in East Antarctica. While this modern spatial slope is of current use for interpreting glacial-interglacial changes (Jouzel et al., 2003, 2007), the magnitude of the variability for present-day or warmer conditions may be underestimated (by typically 30%), as suggested by isotope modelling studies for present day interannual variability (Schmidt et al., 2007) or for projections towards a warmer $CO_2$ world (Sime et al., 2008).

The comparison of the long term trends first allows the characterization of the corresponding multi-millennial climate variability (>5000 years) over the two focused periods and to depict two different evolutions. The Holocene signal exhibits two successive plateaus, one between 10 and 11.7 ka, characterized by a $\delta D$ anomaly of $\sim$+4‰ and the second one from the present day to 5.5 ka, at Holocene mean level. In contrast, MIS 11 presents a slow $\delta D$ increase between 413 and 421 ka, followed by a rapid warming that reaches a $\delta D$ optimum at $\sim$407 ka of $\sim$7‰ above MIS 11 mean value level, before finally entering its cooling phase. The relationship between these long-term trends and the high- frequency climate variability of our two interglacials is then documented by a variance and a spectral analysis, following the methods described in Sects. 3.3 and 3.4.

### 5.1 Variance analysis

By substracting the red signal from the black one (Fig. 2 panels a), one gains access to the millennial to sub-millennial scale variability as represented on panels b of Fig. 2. The remaining signal gives information on the amplitude of variations characteristic of both periods. Even after the correction for isotopic diffusion (see Sect. 3.2), the MIS 11 $\delta D$ signal characterized by a maximal amplitude of variations of $\sim$7‰ does not reach the level of variability exhibited during Holocene (up to $\sim$10‰). This difference partly arises from the Holocene temporal resolution more than twice better than the MIS 11 one. When resampling the Holocene signal every 50 years as done for MIS 11, the amplitude of MIS 1 variation is reduced to 8‰ (not shown).

In order to go beyond the problem of variability levels, we compared the evolution of sub-millennial climate variability (Fig. 2 panels c) by calculating a running standard deviation over 3 ka of the panels b signals (see Sect. 3.3). The lower variability for MIS 11 was again clearly depicted with values oscillating around 2‰ (up to 2.5‰ after back diffusion correction in grey) against 3.5‰ for MIS 1. For the description of the variability evolution, the noticeable points of standard deviation slope changes were labelled by letters ordered from the past to the present. Holocene variability first showed a progressive increase of $\sim$0.6‰ from point 1.A to 1.B. Then, the variability decreased (until the point 1.C) before reaching a quite stable level (albeit with a weak increase during the last 5 ka). The MIS 11 pattern of variability is characterized by a non-stable region followed by a quickly increasing variability (by 1‰ from 11.A to 11.B) with a maximal running standard deviation value of $\sim$2.5‰ hold until the point 1.C. The variability then decreased by 0.5 (from 11.C to 11.D) before progressively increasing again at the end of MIS 11. Except for the overall level of variability, the pattern remained unchanged when taking into account isotopic diffusion (grey curve). Therefore, only the original signal (in black) is discussed in the rest of this study.

These changes of millennial to sub-millennial-scale variability can be linked to the long-term trend by plotting (panels d Fig. 2) the running standard deviation with respect to a running average over 3 kyr of each interglacial $\delta D$ signal trend. This approach highlights the progressive increase of Holocene variability (from 1.A to 1.B) occurring during the cooling phase between the two plateaus. In contrast, its decrease until 1.C is linked to the slow Mid-Holocene warming. For MIS 11, the noticeable increase of variability between 11.A and 11.B begins just before the maximum of the $\delta D$ signal. The highest value of the standard deviation is maintained stable during the beginning of the cooling phase.

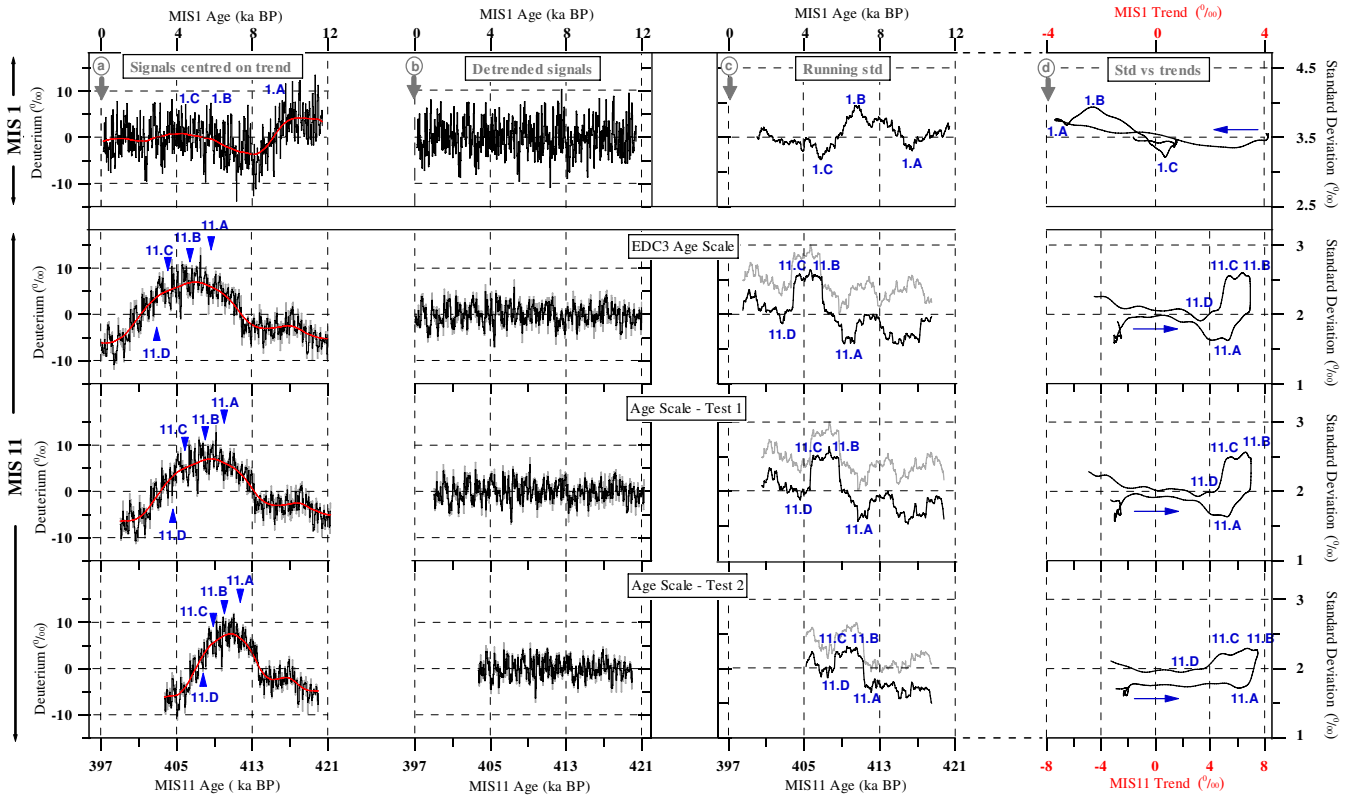


**Fig. 2.** Variability analysis (in ‰) of MIS 1 (top), MIS 11 using EDC3 chronology (middle top), Test 1 age-scale (middle bottom) and Test 2 age-scale (bottom). **(a)** Signals (black) centred on the $\delta D$ mean value of the period focussed on: 0–12 ka for MIS 1; 397–421 ka for MIS 11 – EDC3; 399–421.3 ka for MIS 11 – Test 1; 403.7–420 ka for MIS 11 – Test 2. The general trends are plotted in red; signals corrected from isotopic diffusion in grey for MIS 11. **(b)** Signals minus their respective trends (red, panels a). **(c)** Calculated running standard deviation of panel b signals over 3 kyr, from the past 1.5 kyr to the next 1.5 kyr at a given time point (black: original signals; grey: correction for isotopic diffusion). Remarkable changes of slope are labelled from A to C or D from past to present (the 1 or 11 numbers refer to the studied interglacial). **(d)** Running standard deviation (panels c, ‰) plotted in the function of the respective general trends (panels a, red, ‰). Signals are smoothed using a binomial algorithm for an easier readability. The labelled points (panels c) are reported and arrows indicate the way of reading from past to present.

After an abrupt decrease (from 11.C to 11.D), the variability keeps increasing during the final cooling phase at the end of MIS 11. Despite a symmetrical aspect of the $\delta D$ trend on each side of the MIS 11 optimum (comparable increasing and decreasing trends), the sub-millennial variability exhibits a clear shift between the warming and the cooling phases. MIS 11 thus presents a higher level of variability during all the cooling phases, even after its abrupt decrease (from 11.C to 11.D). This feature is comparable to the Holocene increasing variability observed during the short cooling between its two plateaus. This highlights a difference in terms of climate dynamics between cooling and warming phases.

### 5.2 Spectral analysis

We performed a spectral analysis of the detrended signals (displayed on Fig. 2 panels b, black) for each interglacial focus period using a wavelet analysis (see Sect. 3.4). The difference of temporal resolution between MIS 1 and 11 implies a different available range of frequencies for our two interglacial periods (25 to 10 $kyr^{-1}$ for MIS 1 and 11 respectively corresponding to 40 and 100 year cycles). For the present comparison, we focussed on multi-centennial variability accessible with the 50 year resolution of MIS 11 data. Due to the diffusion (characterized by a ∼8 cm diffusion length at MIS 11 depth, see Sect. 3.2) all the periodicities under ∼130 years were lost in the spectral signal. Figure 3 displays the time-continuous spectra of the two interglacials.

We can first observe a millennial to multi-centennial scale variability for both interglacials. Holocene is marked by significant periodicities from 90 to ∼ 300 years punctually present over the full period. In contrast, the multi-centennial scale variability is not present persistently over the full MIS 11 spectrum but appears from ∼406 ka (based on EDC3 chronology), as revealed by the highlighted significant periodicities ranged between ∼180 to ∼500 years (highlighted I Fig. 3 with a dashed contour). The establishment of this multi-centennial variability is then followed by the

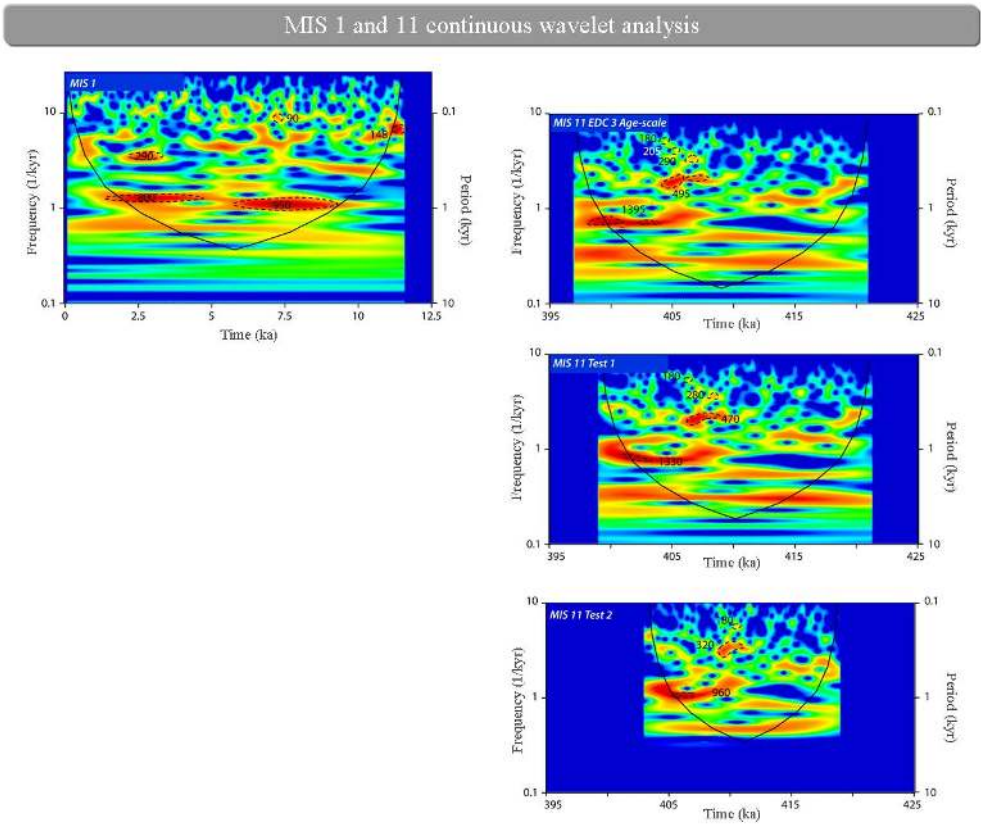


**Fig. 3.** Spectral analysis of the detrended signals (displayed on Fig. 2, panels b) for MIS 1 (left) and MIS 11 (right), using EDC3 chronology (top), Test 1 age-scale (middle) and Test 2 (bottom). The spectral power is displayed in function of time (ka) in term of frequency (1/kyr, left axis) or period (kyr, right axis). Black lines correspond to the cone of influence; dotted lines indicate the significant periodicities (application of the statistical test of Torrence and Compo: http://paos.colorado.edu/research/wavelets/).

occurrence of a ∼1400 year significant periodicity. MIS 11 thus presents a transition in its variability pattern coinciding with the beginning of the long-term cooling phase (Fig. 2a). The previous observation of high amplitudes of variations between 11.B and C points (see Sect. 5.1) can thus be attributed to the onset of multi-centennial variability from ∼406 ka. Then, the variability increasing again after the 11.D point seems to be more strongly expressed at millennial scale. Altogether, these results highlight the establishment of a new mode of climatic variability during the final cooling phase of MIS 11, as first noted in the variance analysis. By comparison, a small transition in the MIS 1 millennial scale variability can be detected at ∼5.5 ka with a ∼950 year periodicity changing into a ∼800 year cycle. This corresponds to the beginning of the second plateau of Holocene (see Fig. 2 panel a), which is also marked by amplitudes of variations progressively decreasing (segment 1.B to 1.C) before reaching a stable level of variability (Sect. 5.1).

### 5.3 Sensitivity to uncertainties on MIS 11 duration

The previous comparison between MIS 1 and 11 climate variability features is constrained by their durations, here based on the EDC3 chronology (Parrenin et al., 2007). Referring to the −403‰ level for the definition of an interglacial in the EDC core (see Sect. 2, EPICA-community-members, 2004), the EDC3 age-scale estimates that MIS 1 has lasted ∼12 kyr so far, consistent with the new EDC chronology established back to 50 ka (Lemieux-Dudon et al., 2010) and derived from a new inverse method for ice core dating (Lemieux-Dudon et al., 2009). The estimate for MIS 11 duration is of ∼32 kyr with a given uncertainty of ±20% (±6.4 kyr). With the added difficulty of comparing different types of records that use different references for delineating the interglacial periods, the Lisiecki and Raymo (2005) chronology for marine sediment cores established the beginning of MIS 1 at ∼11 ka and evaluated the benthic MIS 11 duration of 20 kyr between 398 and 418 ka (with an uncertainty of 4 kyr on absolute ages), suggesting a shorter MIS 11 than depicted in EDC3 for Antarctic temperature. In parallel, Kawamura et al. (2010) have recently extended an orbital

$\delta O_2/N_2$ chronology for the Antarctic Dome Fuji core, first established for the past 360 kyr (Kawamura et al., 2007), back to 470 ka. They obtained a MIS 11 duration shorter by ∼9 kyr in comparison with the EDC3 chronology. Such differences between MIS 11 length estimates lead us to perform sensitivity tests on MIS 11 duration and to evaluate the impacts on MIS 11 climate variability using the same variance and spectral analyses as before (see Sect. 5).

Considering $O_2/N_2$ ratios measured in the trapped air of ice cores as direct tools (free from the usual Δage between gas and ice) for the establishment of orbital tuning chronology (Bender, 2002), we have used EDC $O_2/N_2$ data (Landais et al., 2011) to produce two other age scales for MIS 11 (Fig. 1d and e) in a different way than a simple linear compression of MIS 11 duration. By synchronising the mean 75° S insolation curve to the EDC $O_2/N_2$record arbitrarily (as done in Landais et al., 2011), the first age-scale obtained shortens our MIS 11 signal by ∼4 kyr, now dated between 395.2 and 425.7 ka (Fig. 1d, hereafter Test1). Such a reduced duration was also tested in Rohling et al. (2010) and remains within the uncertainty range of the EDC3 time-scale. A second age-scale test can be then produced by fitting the EDC3 with the orbital Dome Fuji chronology, reducing in larger proportions the MIS11 duration by ∼8.5 kyr, between 400.5 and 426 ka (Fig. 1e, hereafter Test 2).

Focussing on the same part of the MIS 11 signal as in Sect. 5 (Fig. 1d and e, grey areas), the variability is then analysed on the corresponding reduced time-intervals ranging from 399 to 421.3 ka and from 403.7 to 420 ka for Test 1 and 2 (Fig. 2). The impacts of Test 1 on MIS 11 variability analysis are globally negligible compared to the previous results obtained with the EDC3 age-scale. The amplitude of variations (panel b) is hardly affected; the running standard deviation (panel c) and its evolution with respect to trend (panel d) exhibit an overall similar pattern as the one produced using the EDC3 age-sale. In contrast, the significant shortening of the MIS 11 duration by Test 2 drops the level of variability by 1.5‰ (panel b). The running standard deviation is then affected and presents values of 0.3‰ lower on average than using the original signal (panel c). Its evolution with respect to the trend is impacted with less pronounced changes of variability levels (between 11.A and 11.B, 11.C and 11.D, panel d). But, both for Test 1 and Test 2, the panels d illustrate that the main features described in Sect. 5.1 remain unchanged, showing that the age-scale uncertainties do not affect our main conclusions regarding changes in variance.

In parallel, spectral analysis is obviously affected by dating uncertainties, and again with a greater impact when applying Test 2 compared to the use of Test 1 (Fig. 3). Hence, the MIS 11 spectrum obtained by the application of Test 1 first shows a loss of the ∼200-year periodicity previously highlighted with the EDC3 chronology at ∼406 ka; the ∼1400-year one presents a value slightly shifted to ∼1330 years and becomes also more pronounced at the end of the studied period. Second, Test 2 implies fewer significant periodicities at the multi-centennial scale and turns the ∼1400-year periodicity value into ∼950 years. Altogether, our sensitivity tests still exhibit the same pattern of variability and confirm the robustness of a changing climate dynamics at the onset of the final MIS 11 cooling phase.

## 6 Discussion

We now discuss the links between the variability features highlighted in the $\delta D$ signals of MIS 1 and 11, natural climate forcings and internal climate variability. While long-term changes have classically been attributed to the climate system response to orbital forcing (as firstly hypothesised by Milankovitch, 1941), the drivers of millennial to sub-millennial variability involve external forcings such as solar and volcanic activities, as well as internal climate dynamics including the oceanic and atmospheric components (as further discussed in the following sub-sections). In particular, one can question the influence of local processes such as precipitation intermittency, moisture origin, evaporation conditions in relationship with atmospheric circulation and austral ocean surface conditions on the Antarctic $\delta D$ records.

As the Holocene benefits from a substantial documentation, we first discuss the results of MIS 1 spectral analysis in the context of the literature available. Assuming that the patterns of forcings and internal modes of variability described over the last 12 kyrs were also at play during MIS 11, we can then suggest that the same mechanisms were involved during MIS 11. Due to the uncertainties on MIS 11 duration which impact the significant periodicities highlighted in our high-resolution $\delta D$ data, analogy between MIS 1 and 11 climate forcings remains, however, difficult to establish. The discussion is thus limited to the comparison of the general evolutions of MIS 11 $\delta D$ signal and other climate records from different proxies available for the MIS 11 period. .

### 6.1 Spectral Holocene EDC characteristics

By examining the solar activity during the Holocene (as detailed in Steinhilber et al., 2009), we first note that our EDC $\delta D$ Holocene variance (Fig. 2, panel c) cannot simply be explained by changes in solar foricng and deserves further exploration. Spectral analyses of the EDC $\delta D$ signal during the Holocene have already been performed (Yiou et al., 1997; Masson et al., 2000), but without clearly examining the possible relationships with climate actors. Here the wavelet method presents the advantage of being able to mark the onset of the significant periodicities of the Holocene EDC $\delta D$ signal. Then they can be compared to the results of many previous studies that have discussed millennial-to-multi-centennial Holocene variability and its signature in different climate and solar activity records.

The implication of solar forcing in the millennial scale variability of Holocene was first supported by Bond et

al. (1997, 2001). Refering to cosmogenic nucleides ($^{14}$C and $^{10}$Be) measurements, they claimed that the Holocene 1500-year (±500) periodicity found in North Atlantic drift ice records can be attributed to solar forcing. The same periodicity has also been detected in other proxies of the North Atlantic region (Bianchi and McCave, 1999; Campbell et al., 1998; Mayewski et al., 1997 as a non-exhaustive list), as in the Southern Hemisphere (Lamy et al., 2001), but without underlining a persistent link to solar activity. Using the wavelet analysis method on several records from the Northern Hemisphere, Debret et al. (2007) actually highlight a decoupling of the apparent Holocene 1500-year climatic cycle into three superimposed significant periodicities of 1000, 1500 and 2500 years. Whereas the comparison of different marine sediment cores (Bianchi and McCave, 1999; Chapman and Shackleton, 2000; Giraudeau et al., 2000) preferentially attributes the ∼1500-year periodicity to oceanic dynamics, the link between 1000 and 2500-year climatic cycles and solar activity is confirmed when confronting the spectral analyses of Bond et al. (2001) records and of the Vonmoos et al. (2006) $^{10}$Be data,.

Exhibiting cyclicities close to ∼1000 years, our EDC Holocene $\delta D$ record (Fig. 3) could also corroborate the solar forcing at millennial scale in the Antarctic region. But, the spectral analysis actually highlights a decoupling of the ∼1000-year cycle into a ∼950-year periodicity during early Holocene (similar to the Northern records of Bond et al., 2001 and Vonmoos et al., 2006 according to the Debret et al., 2007 analysis and close to the 900-year cycle of Lamy et al., 2001 in the South), to a ∼800-year one in the late Holocene (also recorded in Chapman and Shackleton, 2000). This transition phase in the frequency domain, recorded at ∼5.5 ka in our EDC $\delta D$ signal and phasing with the establishment of a progressive stable level of variability (see Sect. 5.2), was documented in Debret et al. (2009) and Wirtz et al. (2010), in a synthesis of records covering the two Hemispheres. Known as Mid-Holocene transition, it is first suggested by Debret et al. (2009) to underline a change in the dominant mechanisms of variability, from an external origin (essentially from solar activity) in the early Holocene, to internal processes in the late Holocene. This hypothesis is in line with other studies (Wanner et al., 2008; Wirtz et al. 2010), which noticed a lower magnitude of solar variability in the early Holocene compared to the mid to late Holocene. At the same time, Wirtz et al. (2010) observe the emergence of a more pronounced variability at centennial scale (between 200 and 850 years), after this Mid-Holocene transition. Our signal does exhibit a 290-year periodicity (Fig. 3) in the early Holocene. Thus, the establishment of a new mode of variability during the mid Holocene also has to be explored at multi-centennial scale. This leads us to now discuss the possible mechanisms (internal and/or external) at play in the second part of Holocene that could explain the identified multi-centennial variability.

The multi-centennial variability recorded in the Holocene EDC $\delta D$ signal is a common feature of both North and South Hemisphere records. In particular our periodicity of ∼290 years is close to the ∼250-year one found in a East Antarctica marine core (Crosta et al., 2007) at ∼2.5 ka and to the ∼240-year cycle of the Rousse et al. (2006) data from a North Icelandic marine sediment core, identified at ∼3 ka. Climate models (Park and Latif, 2008; Schulz et al., 2007) show that the multi-centennial variability is a persistent feature of Atlantic Ocean circulation. Park and Latif (2008) have demonstrated the implication of both hemispheres in high frequency variability through large changes in the Atlantic sea ice extent, with a rapid response of the Northern Hemisphere at decadal scale and a slower one of the Southern Hemisphere at multi-centennial scale.

Invoking a sun-ocean-climate linkage, Hu et al. (2003) underlined the possible forcing of the multi-centennial changes in the sea ice extent by the centennial solar forcing (Karlén and Kuylenstierna, 1996). The same forcing was further proposed by Varma et al. (2010) to drive the southern annular mode. Altogether, these studies suggest that the multi-centennial scale variability found in the EDC $\delta D$ record could be closely associated with changes in austral sea ice extent and atmospheric circulation, in response to multi-centennial variations in solar activity. Changes in volcanic forcing may also be at play (Castellano et al., 2005), as recent modelling studies suggest a possible centennial response time (Stenchikov et al., 2009; Schneider et al., 2009), but have not yet been explored due to the lack of quantitative reconstructions beyond the last millennium (Gao et al., 2008).

Nevertheless, centennial variability may not necessarily be driven by external forcings and may also result from modes of internal climate variability. Modelling experiments focussing on the North Atlantic Deep Water (NADW) formation (Jongma et al., 2007; Renssen et al., 2007) have indeed highlighted the possibility that internal periodic processes such as freshwater releases could provide a sensible mechanism to explain Holocene multi-centennial scale variability. Focussing on the thermohaline structure of the Southern Ocean, Pierce et al. (1995) also linked modelled centennial-scale oscillations with changes both in the local precipitation affecting the Antarctic Circumpolar Current and in the NADW.

Thus, while bipolar see-saw patterns are well known to link Antarctica and Greenland, stable isotope records during abrupt glacial (Blunier et al., 1998) or early interglacial events (Masson-Delmotte et al., 2010), even at sub-millennial scale (Capron et al., 2010), these modelling experiments reinforce the hypothesis of a similar interhemispheric linkage at play in multi-centennial variability during interglacial periods. Such internal mechanisms could be involved in the observed variability changes at the Mid-Holocene transition, as previously suggested by Debret et al. (2009).

### 6.2 MIS 11 EDC variability

Here the spectral analysis of MIS 11 cannot be discussed in the same way as for MIS 1, due to large uncertainties on MIS 11 duration and the absence of information about external forcings (solar and volcanic activities) for this period. The MIS 11 still benefits from sufficient documentation to allow comparisons between our new EDC $\delta D$ profile and "other" proxy signals.

In addition to various climatic information provided by the EDC core (e.g. Jouzel et al., 2007; Siegenthaler et al., 2005; Spahni et al., 2005), MIS 11 has been documented in other long marine or continental records through different proxies (Lisiecki and Raymo, 2005; McManus et al., 2003; Tzedakis et al., 2006). They consistently underline the general comparable background climate conditions between MIS 1 and 11 (e.g. sea level, greenhouse gas concentrations, local temperatures, vegetation history) and the exceptional length of MIS 11. One study (de Vernal and Hillaire-Marcel, 2008) emphasizes an exceptional development of boreal ecosystems on the Greenland coasts, suggesting particularly reduced Greenland ice sheet extent during this interglacial. Due to the lack of a sufficient temporal resolution for performing reliable spectral analysis, comparisons with these records remain, however, restricted to the analyses of trends or intensities.

Still, similarities between the EDC $CO_2$ (Siegenthaler et al., 2005) and the 500-year resolution $\delta^{13}C$ record of a marine core from the Cape Basin (Dickson et al., 2008) at the end of MIS 11 have revealed an interesting oceanic circulation - atmospheric $CO_2$ concentration linkage. The parallel between the observed $\delta^{13}C$ gradient and $CO_2$ drawdown at the end of MIS 11 supports the hypothesis of a close link between deep austral ocean ventilation and changes in atmospheric greenhouse gas concentrations (Toggweiler, 1999; Hodell et al., 2003). The onset of an increasing variability in our $\delta D$ record (at ∼406 ka) does not coincide with any marked change in the $CO_2$concentration. Its phasing with a methane concentration starting to decrease (Loulergue et al., 2008) and the increase of the EDC sea salt sodium flux (Wolff et al., 2010) is, however, robust within age-scale uncertainties. It suggests that the observed increase in EDC $\delta D$ variability at the end of MIS 11 occurred in parallel to: first, an East Antarctic cooling trend; second, an extent of austral sea ice cover associated with a reduced methane production in tropical and boreal wetlands.

Further discussions about the links between the EDC climate variability (derived from our $\delta D$ data) and ocean circulation variability requires both higher resolution marine records and improved chronologies and synchronization methods. But, as a first step in the MIS 11 variability analysis, our data enables us to suggest that the increased Antarctic variance and the onset of millennial to sub-millennial variability are intimately linked with the global transition between interglacial and glacial states.

## 7 Conclusions

Our $\delta D$ measurements conducted on high-resolution EDC samples have first confirmed the patterns of East Antarctic temperatures over the full MIS 11 period, as previously described by the original $\delta D$ bag record. Then, our study has aimed to demonstrate the added value of analysing EDC high-resolution $\delta D$ data at first, improving the documentation of past interglacial climate variability, going beyond trend and intensity considerations, and second, permitting a comparison with Holocene.

Our results highlight a specific variability pattern during MIS 11 with two distinguishable evolutions on each side of the late MIS 11 maximum (∼406 ka according to the EDC3 chronology). Indeed, the MIS 11 signal is characterized by a variability enhanced from the beginning of the cooling phase, which contrasts with the lower variability exhibited during the preceding warming phase. Moreover, a spectral analysis allows us to relate these MIS 11 variability features with the onset at ∼406 ka of new climatic dynamic modes marked by the emergence of periodicities at millennial to multi-centennial scales.

The Holocene signal exhibits a similar pattern with increasing variability occurring just after the early Holocene plateau and persistent during the following decrease in temperatures. Unlike that for MIS11, this change in variance is not evidenced in the spectral analysis. The Mid-Holocene transition, dated at 5.5 ka and documented in many previous studies, is still imprinted in the obtained spectrum and characterized by a shift in the significant periodicities.

The links between Holocene variability changes on each side of this transition and external forcings or internal climate system responses can be explored, thanks to the limited uncertainties (∼100–200 years) on Holocene EDC dating and the substantial available documentation. Such discussion is, however, impossible for the MIS 11 signal, because of the lack of records with sufficient resolution, the lack of documentation of natural forcing variability, and because of the large age-scale uncertainties attached to the MIS 11 duration. While our results about MIS 11 variability patterns are robust with respect to these uncertainties, the length of MIS 11 impacts in a larger proportion the values of periodicities revealed by the spectral analysis. It thus prevents the clear attribution of the increasing variability at the glacial inception to one or other climatic component.

Consequently, we stress the need to: first scrutinize the MIS 11 variability with other records, e.g. from tropical, temperate and polar regions at sufficient temporal resolution for improving the global documentation of changes in variability along the full period; second, reduce uncertainties on the length of this interglacial by building an accurate reference time-scale for the EDC core. It will help in the future to precisely specify the MIS 11 variability spectrum, but also that of other past interglacials. New detailed isotopic measurements from the EDC core are indeed now available for a

variety of interglacials and will allow the further exploration ofthe relationships between mean state and Antarctic climate variability under contrasted orbital contexts.

**Supplementary material related to this article is available online at: http://www.clim-past.net/7/437/2011/cp-7-437-2011-supplement.zip.**

*Acknowledgements.* The authors wish to thank C. Lemmen and M. Mudelsee for their interest in the present study and their constructive reviews which helped us to improve this article. This work is a contribution to the European Project for Ice Coring in Antarctica (EPICA), a joint European Science Foundation/European Commission scientific programme, funded by the EU and by national contributions from Belgium, Denmark, France, Germany, Italy, the Netherlands, Norway, Sweden, Switzerland and the United Kingdom. The main logistic support was provided by IPEV and PNRA (at Dome C) and AWI (at Dronning Maud Land). This work also contributes to the HOLOCLIP project, a joint research project of the ESF PolarCLIMATE programme, funded by national contributions from Italy, France, Germany, Spain, The Netherlands, Belgium and the United Kingdom. The research leading to these results has in particular received funding from the European Union's Seventh Framework programme (FP7/2007–2013) under grant agreement no 243908, "Past4Future, Climate change – Learning from the past climate". This is EPICA publication 275, HOLOCLIP publication 2, Past4Future contribution 6 and LSCE publication 4512.

Edited by: G. Lohmann


The publication of this article has been financed by CNRS-INSU.

## References

Bender, M. L.: Orbital tuning chronology for the Vostok climate record supported by trapped gas composition, Earth Planet. Sc. Lett., 204, 275–289, 2002.

Bianchi, G. G. and McCave, I. N.: Holocene periodicity in North Atlantic climate and deep-ocean flow south of Iceland, Nature, 397, 515–517, 1999.

Bintanja, R., van de Wal, R., and Oerlemans, J.: Modelled atmospheric temperatures and global sea levels over the past million years, Nature, 437, 125–128, 2005.

Blunier, T., Chappellaz, J., Schwander, J., Dallenbäch, A., Stauffer, B., Stocker, T., Raynaud, D., Jouzel, J., Clausen, H. B., Hammer, C. U., and Johnsen, S. J.: Asynchrony of Antarctic and Greenland climate change during the last glacial period., Nature, 394, 739–743, 1998.

Bond, G., Showers, W., Cheseby, M., Lotti, R., Almasi, P., deMenocal, P., Priore, P., Cullen, H., Hajdas, I., and Bonami, G.: A pervasive millennial-scale cycle in the north atlantic Holocene and glacial climates, Science, 278, 1257–1266, 1997.

Bond, G., Kromer, B., Beer, J., Muscheler, R., Evans, M. N., Showers, W., Hoffmann, S., Lotti-Bond, R., Hajdas, I., and Bonani, G.: Persistent solar influence on north Atlantic climate during the Holocene, Science, 294, 2130–2136, 2001.

Bowen, D. Q.: Sea level ∼400 000 years ago (MIS 11): analogue for present and future sea-level?, Clim. Past, 6, 19–29, doi:10.5194/cp-6-19-2010, 2010.

Campbell, I. D., Campbell, C., Apps, M. J., Rutter, N. W., and Bush, A. B. G.: Late Holocene ∼1500 yr climatic periodicities and their implications, Geology, 26, 471–473, 1998.

Capron, E., Landais, A., Chappellaz, J., Schilt, A., Buiron, D., Dahl-Jensen, D., Johnsen, S. J., Jouzel, J., Lemieux-Dudon, B., Loulergue, L., Leuenberger, M., Masson-Delmotte, V., Meyer, H., Oerter, H., and Stenni, B.: Millennial and sub-millennial scale climatic variations recorded in polar ice cores over the last glacial period, Clim. Past, 6, 345–365, doi:10.5194/cp-6-345-2010, 2010.

Castellano, E., Becagli, S., Hansson, M., Hutterli, M., Petit, J. R., Rampino, M. R., Severi, M., Steffensen, J. P., Traversi, R., and Udisti, R.: Holocene volcanic history as recorded in the sulfate stratigraphy of the European Project for Ice Coring in Antarctica Dome C (EDC96) ice core, J. Geophys. Res., 110, D06114, doi:10.1029/2004jd005259, 2005.

Chapman, M. R. and Shackleton, N. J.: Evidence of 550-year and 1000-year cyclicities in North Atlantic circulation patterns during the Holocene, The Holocene, 10, 287–291, 2000.

Crosta, X., Debret, M., Denis, D., Courty, M. A., and Ther, O.: Holocene long- and short-term climate changes off Adélie Land, East Antarctica, Geochem. Geophys. Geosyst., 8, Q11009, doi:10.1029/2007gc001718, 2007.

Crosta, X., Debret, M., Denis, D. Courty, M. A., and Ther, O.: Holocene long- and short-term climate changes off Adélie Land, East Antarctica, Geochem. Geophy. Geosy., 8, Q11009, doi:10.1029/2007gc001718, 2007.

de Vernal, A. and Hillaire-Marcel, C.: Natural Variability of Greenland Climate, Vegetation, and Ice Volume During the Past Million Years, Science, 320, 1622–1625, doi:10.1126/science.1153929, 2008.

Debret, M., Bout-Roumazeilles, V., Grousset, F., Desmet, M., McManus, J. F., Massei, N., Sebag, D., Petit, J.-R., Copard, Y., and Trentesaux, A.: The origin of the 1500-year climate cycles in Holocene North-Atlantic records, Clim. Past, 3, 569–575, doi:10.5194/cp-3-569-2007, 2007.

Debret, M., Sebag, D., Crosta, X., Massei, N., Petit, J. R., Chapron, E., and Bout-Roumazeilles, V.: Evidence from wavelet analysis for a mid-Holocene transition in global climate forcing, Quat. Sci. Rev., 28, 2675–2688, 2009.

Dickson, A. J., Leng, M. J., and Maslin, M. A.: Mid-depth South Atlantic ocean circulation and chemical stratification during MIS-10 to 12: implications for atmospheric $CO_2$, Clim. Past Discuss., 4, 667–695, doi:10.5194/cpd-4-667-2008, 2008.

Ekaykin, A. A., Lipenkov, V. Y., Barkov, N. I., Petit, J. R., and Masson-Delmotte, V.: Spatial and temporal variability in isotope composition of recent snow in the vicinity of Vostok Station: implications for ice-core record interpretation, Ann. Glaciol., 35,

181–186, 2002.

EPICA-community-members: Eight glacial cycles from an Antarctic ice core, Nature, 429, 623–628, 2004.

Gao, C., Robock, A., and Ammann, C.: Volcanic forcing of climate over the past 1500 years: An improved ice core-based index for climate models, J. Geophys. Res., 113, D23111, doi:10.1029/2008jd010239, 2008.

Giraudeau, J., Cremer, M., Manthé, S., Labeyrie, L., and Bond, G.: Coccolith evidence for instabilities in surface circulation south of Iceland during Holocene times, Earth Planet. Sc. Lett., 179, 257–268, 2000.

Hodell, D. A., Venz, K. A., Charles, C. D., and Ninnemann, U. S.: Pleistocene vertical carbon isotope and carbonate gradients in the South Atlantic sector of the Southern Ocean, Geochem. Geophy. Geosy., 4, 1–19, doi:10.1029/2002GC000367, 2003.

Hu, F. S., Kaufman, D., Yoneji, S., Nelson, D., Shemesh, A., Huang, Y., Tian, J., Bond, G., Clegg, B., and Brown, T.: Cyclic Variation and Solar Forcing of Holocene Climate in the Alaskan Subarctic, Science, 301, 1890–1893, doi:10.1126/science.1088568, 2003.

IPCC: Climate Change 2007 – The Physical Science Basis, Fourth Assessment Report, edited by: Change, I. P. o. C., Cambridge University Press, Cambridge, 1009 pp., 2007.

Johnsen, S. J.: Stable Isotope Homogenization of Polar Firn and Ice, from the International Symposium on Isotopes and Impurities in Snow and Ice, Proceedings IU66 Symposium 118, pp. 210-219, http://iahs.info/redbooks/a118/iahs_118_0210.pdf, 1977.

Johnsen, S. J., Clausen, H. B., Cuffey, K. M., Hoffmann, G., Schwander, J., and Creyts., T.: Diffusion of stable isotopes in polar firn and ice: the isotope effect in firn diffusion, Physics of ice core records, edited by: Hondoch T., Sapporo, Hokkaido University Press, 121–140, 2000.

Jongma, J. I., Prange, M., Renssen, H., and Schulz, M.: Amplification of Holocene multicentennial climate forcing by mode transitions in North Atlantic overturning circulation, Geophys. Res. Lett., 34, L15706, doi:10.1029/2007gl030642, 2007.

Jouzel, J., Vaikmae, R., Petit, J. R., Martin, M., Duclos, Y., Stiévenard, M., Lorius, C., Toots, M., A., M. M., Burckle, L. H., Barkov, N. I., and Kotlyakov, V. M.: The two-step shape and timing of the last deglaciation in Antarctica, Clim. Dyn., 11, 151–161, 1995.

Jouzel, J., Masson, V., Cattani, O., Falourd, S., Stievenard, M., Stenni, B., Longinelli, A., Johnsen, S. J., Steffenssen, J. P., Petit, J. R., Schwander, J., Souchez, R., and Barkov, N. I.: A new 27 Ky high resolution East Antarctic climate record, Geophys. Res. Lett., 28, 3199–3202, 2001.

Jouzel, J., Vimeux, F., Caillon, N., Delaygue, G., Hoffmann, G., Masson-Delmotte, V., and Parrenin, F.: Magnitude of the isotope-temperature scaling for interpretation of central Antarctic ice cores, J. Geophys. Res., 108, 1029–1046, 2003.

Jouzel, J., Masson-Delmotte, V., Cattani, O., Dreyfus, G., Falourd, S., Hoffmann, G., Minster, B., Nouet, J., Barnola, J. M., Chappellaz, J., Fischer, H., Gallet, J. C., Johnsen, S., Leuenberger, M., Loulergue, L., Luethi, D., Oerter, H., Parrenin, F., Raisbeck, G., Raynaud, D., Schilt, A., Schwander, J., Selmo, E., Souchez, R., Spahni, R., Stauffer, B., Steffensen, J. P., Stenni, B., Stocker, T. F., Tison, J. L., Werner, M., and Wolff, E.: Orbital and millenial Antarctic climate variability over the past 800,000 years, Science 317, 793–796, 2007.

Karlén, W. and Kuylenstierna, J.: On solar forcing of Holocene climate: evidence from Scandinavia, The Holocene, 6, 359–365, 1996.

Kawamura, K., Parrenin, F., Lisiecki, L., Uemura, R., Vimeux, F., Severinghaus, J. P., Hutterli, M. A., Nakazawa, T., Aoki, S., Jouzel, J., Raymo, M. E., Matsumoto, K., Nakata, H., Motoyama, H., Fujita, S., Goto-Azuma, K., Fujii, Y., and Watanabe, O.: Northern Hemisphere forcing of climatic cycles in Antarctica over the past 360,000 years, Nature, 448, 912–915, 2007.

Kawamura, K., Aoki, S., Nakazawa, T., Abe-Ouchi, A., and Saito, F.: Timing and duration of the last five interglacial periods from an accurate age model of the Dome Fuji Antarctic ice core, AGU Meeting, 2010.

Lamy, F., Hebbeln, D., Röhl, U., and Wefer, G.: Holocene rainfall variability in southern Chile: a marine record of latitudinal shifts of the Southern Westerlies, Earth Planet. Sc. Lett., 185, 369–382, 2001.

Landais, A., Dreyfus, G., Capron, E., Pol, K., Loutre, M.-F., Raynaud, D., Lipenkov, V. Y., Masson-Delmotte, V., Jouzel, J., and Leuenberger, M.: On the limits of orbital dating using EPICA Dome C $\delta O_2/N_2$, revised, 2011.

Lemieux-Dudon, B., Parrenin, F., and Blayo, E.: A probalistic method to construct an optimal ice chronology for ice cores, Physics of Ice Core Records II, 68, 2009.

Lemieux-Dudon, B., Blayo, E., Petit, J.-R., Waelbroeck, C., Svensson, A., Ritz, C., Barnola, J.-M., Narcisi, B. M., and Parrenin, F.: Consistent dating for Antarctic and Greenland ice cores, Quaternary Sci. Rev., 29, 8–20, doi:10.1016/j.quascirev.2009.11.010, 2010.

Lisiecki, L. E. and Raymo, M. E.: A Pliocene-Pleistocene stack of 57 globally distributed benthic d18O records, Paleoceanography, 20, doi:10.1029/2004PA001071, 2005.

Loulergue, L., Schilt, A., Spahni, R., Masson-Delmotte, V., Blunier, T., Lemieux, B., Barnola, J. M., Raynaud, D., Stocker, T., and Chappelaz, J.: Orbital and millenial-scale features of atmospheric $CH_4$ over the last 800 000 years, Nature, 453, 383–386, 2008.

Loutre, M. F. and Berger, A.: Future Climatic Changes: Are We Entering an Exceptionally Long Interglacial?, Clim. Change, 46, 61–90, 2000.

Loutre, M. F. and Berger, A.: Marine isotope stage 11 as an analogue for the present interglacial, Glob. Planet. Change, 36, 209–217, 2003.

Lüthi, D., Floch, M. L., Bereiter, B., Blunier, T., Barnola, J. M., Siegenthaler, U., Raynaud, D., Jouzel, J., Fischer, H., Kawamura, K., and Stocker, T. F.: High resolution carbon dioxide concentration record 650 000–800 000 years before present, Nature, 453, 379–382, 2008.

Masson-Delmotte, V., Stenni, B., Blunier, T., Cattani, O., Chappellaz, J., Cheng, H., Dreyfus, G., Edwards, R. L., Falourd, S., Govin, A., Kawamura, K., Johnsen, S. J., Jouzel, J., Landais, A., Lemieux-Dudon, B., Lourantou, A., Marshall, G., Minster, B., Mudelsee, M., Pol, K., Röthlisberger, R., Selmo, E., and Waelbroeck, C.: Abrupt change of Antarctic moisture origin at the end of Termination II, P. Natl. Acad. Sci. USA, 107(27) 12091–12094, doi:10.1073/pnas.0914536107, 2010.

Masson-Delmotte, V., Stenni, B., and Jouzel, J.: Common millenial scale variability of Antarctic and Southern Ocean temperatures during the past 5000 years reconstructed from EPICA Dome C

ice core, The Holocene, 14, 145–151, 2004.

Masson-Delmotte, V., Dreyfus, G., Braconnot, P., Johnsen, S., Jouzel, J., Kageyama, M., Landais, A., Loutre, M.-F., Nouet, J., Parrenin, F., Raynaud, D., Stenni, B., and Tuenter, E.: Past temperature reconstructions from deep ice cores: relevance for future climate change, Clim. Past, 2, 145–165, doi:10.5194/cp-2-145-2006, 2006.

Masson-Delmotte, V., Hou, S., Ekaykin, A., Jouzel, J., Aristarain, A., Bernardo, R. T., Bromwhich, D., Cattani, O., Delmotte, M., Falourd, S., Frezzotti, M., Gallée, H., Genoni, L., Isaksson, E., Landais, A., Helsen, M., Hoffmann, G., Lopez, J., Morgan, V., Motoyama, H., Noone, D., Oerter, H., Petit, J. R., Royer, A., Uemura, R., Schmidt, G. A., Schlosser, E., Simões, J. C., Steig, E., Stenni, B., Stievenard, M., Broeke, M. v. d., Wal, R. v. d., Berg, W.-J. v. d., Vimeux, F., and White, J. W. C.: A review of Antarctic surface snow isotopic composition : observations, atmospheric circulation and isotopic modelling, J. Climate, 21, 3359–3387, 2008.

Masson, V., Vimeux, F., Jouzel, J., Morgan, V., Delmotte, M., Ciais, P., Hammer, C., Johnsen, S., Lipenkov, V. Y., Mosley-Thompson, E., Petit, J.-R., Steig, E., Stievenard, M., and Vaikmae, R.: Holocene climate variability in Antarctica based on 11 ice-core isotopic records, Quaternary. Res., 54, 348–358, 2000.

Mayewski, P. A., Meeker, L. D., Twickler, M. S., Whitlow, S., Yang, Q., Lyons, W. B., and Prentice, M.: Major features and forcing of high-latitude northern hemisphere atmospheric circulation using a 110,000-year-long glaciochemical series, J. Geophys. Res., 102, 26345–26366, doi:10.1029/96jc03365, 1997.

McManus, J. F., Oppo, J., Callen, J., and Healey, S.: Marine Isotope Stage 11 (MIS 11): Analog for Holocene and future climate?, Geoph. Monog. Series, 137, 69–85, 2003.

Milankovitch, M.: Canon of Insolation and the Ice Age Problem, Belgrade: Zavod za UdzÌE benike i Nastavna Sredstva, 1941 (1998).

Mudelsee M (2010) Climate Time Series Analysis: Classical Statistical and Bootstrap Methods. Springer, Dordrecht Heidelberg London New York. [ISBN-13: 978-90-481-9481-0, ISBN-10: 90-481-9481-4, e-ISBN: 978-90-481-9482-7, DOI: 10.1007/978-90-481-9482-7; approximately xxxiv + 474 pp; Atmospheric and Oceanographic Sciences Library, Vol. 42]

Mudelsee M.: Climate Time Series Analysis: Classical Statistical and Bootstrap Methods. Springer, Dordrecht Heidelberg London New York, (www.manfredmudelsee.com/book), ISBN-13: 978-90-481-9481-0, ISBN-10: 90-481-9481-4, e-ISBN: 978-90-481-9482-7, doi:10.1007/978-90-481-9482-7; approximately xxxiv + 474 pp; Atmospheric and Oceanographic Sciences Library, Vol. 42, 2010.

Neumann, T. A. and Waddington, E. D.: Effects of firn ventilation on isotopic exchange, J. Glaciol., 169, 183–194, 2004.

Park, W. and Latif, M.: Multidecadal and multicentennial variability of the meridional overturning circulation, Geophys. Res. Lett., 35, L22703, doi:10.1029/2008gl035779, 2008.

Parrenin, F., Barnola, J.-M., Beer, J., Blunier, T., Castellano, E., Chappellaz, J., Dreyfus, G., Fischer, H., Fujita, S., Jouzel, J., Kawamura, K., Lemieux-Dudon, B., Loulergue, L., Masson-Delmotte, V., Narcisi, B., Petit, J.-R., Raisbeck, G., Raynaud, D., Ruth, U., Schwander, J., Severi, M., Spahni, R., Steffensen, J. P., Svensson, A., Udisti, R., Waelbroeck, C., and Wolff, E.: The EDC3 chronology for the EPICA Dome C ice core, Clim. Past, 3, 485–497, doi:10.5194/cp-3-485-2007, 2007.

Pierce, D. W., Barnett, T. P., and Mikolajewicz, U.: Competing Roles of Heat and Freshwater Flux in Forcing Thermohaline Oscillations, J. Phys. Oceanogr., 25, 2046–2064, 1995.

Pol, K., Masson-Delmotte, V., Johnsen, S., Bigler, M., Cattani, O., Durand, G., Falourd, S., Jouzel, J., Minster, B., Parrenin, F., Ritz, C., Steen-Larsen, H. C., and Stenni, B.: New MIS 19 EPICA Dome C high resolution deuterium data: hints for a problematic preservation of climate variability in the "oldest ice", Earth Planet. Sc. Lett., doi:10.1016/j.epsl.2010.07.030, 2010.

Ramseier, R. O.: Self-Diffusion of Tritium in Natural and Synthetic Ice Monocrystals, J. Appl. Phys., 38, 2553–2556, 1967.

Renssen, H., Goosse, H., and Fichefet, T.: Simulation of Holocene cooling events in a coupled climate model, Quaternary Sci. Rev., 26, 2019–2029, 2007.

Rohling, E. J., Braun, K., Grant, K., Kucera, M., Roberts, A. P., Siddall, M., and Trommer, G.: Comparison between Holocene and Marine Isotope Stage-11 sea-level histories, Earth Planet. Sc. Lett., 291, 97–105, 2010.

Rousse, S., Kissel, C., Laj, C., Eiríksson, J., and Knudsen, K. L.: Holocene centennial to millennial-scale climatic variability: Evidence from high-resolution magnetic analyses of the last 10 cal kyr off North Iceland (core MD99-2275), Earth Planet. Sc. Lett., 242, 390–405, 2006.

Ruddiman, W. F.: The early anthropogenic hypothesis: Challenges and responses, Rev. Geophys., 45, RG4001, doi:10.1029/2006rg000207, 2007.

Ruddimann, W.: Cold climate during the closest stage 11 analog to recent millennia, Quaternary Sci. Rev., 24, 1111–1121, 2005.

Schmidt, G. A., Legrande, A., and Hoffmann, G.: Water isotope expressions of intrinsic and forced variability in a coupled ocean-atmosphere model, J. Geophys. Res., 112, D10103, 18 pp., doi:10.1029/2006JD007781, 2007.

Schneider, D. P., Ammann, C. M., Otto-Bliesner, B. L., and Kaufman, D. S.: Climate response to large, high-latitude and low-latitude volcanic eruptions in the Community Climate System Model, J. Geophys. Res., 114, D15101, doi:10.1029/2008jd011222, 2009.

Schulz, M., Prange, M., and Klocker, A.: Low-frequency oscillations of the Atlantic Ocean meridional overturning circulation in a coupled climate model, Clim. Past, 3, 97–107, doi:10.5194/cp-3-97-2007, 2007.

Siegenthaler, U., Stocker, T. F., Monnin, E., Lüthi, D., Schwander, J., Stauffer, B., Raynaud, D., Barnola, J.-M., Fischer, H., Masson-Delmotte, V., and Jouzel, J.: Stable carbon cycle-climate relationship during the last Pleistocene, Science, 310, 1313-1317, 2005.

Sime, L. C., Tindall, J. C., Wolff, E. W., Connolley, W. M., and Valdes, P. J.: Antarctic isotopic thermometer during a $CO_2$ forced warming event, J. Geophys. Res., 113, D24119, doi:10.1029/2008jd010395, 2008.

Spahni, R., Chappellaz, J., Stocker, T. F., Loulergue, L., Hausammann, G., Kawamura, K., Flückiger, J., Schwander, J., Raynaud, D., Masson-Delmotte, V., and Jouzel, J.: Variations of atmospheric methane and nitrous oxide during the last 650,000 years from Antarctic ice cores, Science 310, 1317–1321, 2005.

Steinhilber, F., Beer, J., and Fröhlich, C.: Total solar irradiance during the Holocene, Geophys. Res. Lett., 36, L19704, doi:10.1029/2009gl040142, 2009.

Stenchikov, G., Delworth, T. L., Ramaswamy, V., Stouffer, R. J., Wittenberg, A., and Zeng, F.: Volcanic signals in oceans, J. Geophys. Res., 114, D16104, doi:10.1029/2008jd011673, 2009.

Thomson, D.: Time series analysis of Holocene climate data. Phil. Trans. R. Soc. London B, 330(1615), 601–616, 1990.

Toggweiler, J. R.: Variation of Atmospheric $CO_2$ by Ventilation of the Ocean’s Deepest Water, Paleoceanography, 14, 571–588, doi:10.1029/1999pa900033, 1999.

Torrence, C. and Compo, G. P.: A practical guide to wavelet analysis, B. Am. Meteorol. Soc., 79, 61–78, 1998.

Tzedakis, P. C., Hooghiemstra, H., and Pälike, H.: The last 1.35 million years at Tenaghi Philippon: revised chronostratigraphy and long-term vegetation trends, Quaternary Sci. Rev., 25, 3416–3430, 2006.

Tzedakis, P. C., Raynaud, D., McManus, J. F., Berger, A., Brovkin, V., and Kiefer, T.: Interglacial diversity, Nat. Geosci, 2, 751–755, 2009.

Tzedakis, P. C.: The MIS 11 - MIS 1 analogy, southern European vegetation, atmospheric methane and the "early anthropogenic hypothesis", Clim. Past, 6, 131–144, doi:10.5194/cp-6-131-2010, 2010.

Varma, V., Prange, M., Lamy, F., Merkel, U., and Schulz, M.: Solar-forced shifts of the Southern Hemisphere Westerlies during the late Holocene, Clim. Past Discuss., 6, 369–384, doi:10.5194/cpd-6-369-2010, 2010.

Vaughn, B., White, J. W. C., Delmotte, M., Trolier, M., Cattani, O., and Stievenard, M.: An automated system for the uranium reduction method of hydrogen isotope analysis of water, Chem. Geol., 152, 309–319, 1998.

Vonmoos, M., Beer, J., and Muscheler, R.: Large variations in Holocene solar activity: Constraints from 10Be in the Greenland Ice Core Project ice core, J. Geophys. Res., 111, A10105, doi:10.1029/2005ja011500, 2006.

Waelbroeck, C., Labeyrie, L., Michel, E., Duplessy, J. C., McManus, J. F., Lambeck, K., Balbon, E., and Labracherie, M.: Sea-level and deep water temperature changes derived from benthic foraminifera isotopic records, Quaternary Sci. Rev., 21, 295–305, 2002.

Wanner, H., Beer, J., Bütikofer, J., Crowley, T. J., Cubasch, U., Flückiger, J., Goosse, H., Grosjean, M., Joos, F., Kaplan, J. O., Küttel, M., Müller, S. A., Prentice, I. C., Solomina, O., Stocker, T. F., Tarasov, P., Wagner, M., and Widmann, M.: Mid- to Late Holocene climate change: an overview, Quat. Sci. Rev., 27, 1791–1828, 2008.

Wirtz, K. W., Lohmann, G., Bernhardt, K., and Lemmen, C.: Mid-Holocene regional reorganization of climate variability: Analyses of proxy data in the frequency domain, Palaeo 3, 298/3-4, 189–200, http://dx.doi.org/10.1016/j.palaeo.2010.09.019, 2010.

Wolff, E. W., Barbante, C., Becagli, S., Bigler, M., Boutron, C. F., Castellano, E., de Angelis, M., Federer, U., Fischer, H., Fundel, F., Hansson, M., Hutterli, M., Jonsell, U., Karlin, T., Kaufmann, P., Lambert, F., Littot, G. C., Mulvaney, R., Röthlisberger, R., Ruth, U., Severi, M., Siggaard-Andersen, M. L., Sime, L. C., Steffensen, J. P., Stocker, T. F., Traversi, R., Twarloh, B., Udisti, R., Wagenbach, D., and Wegner, A.: Changes in environment over the last 800,000 years from chemical analysis of the EPICA Dome C ice core, Quaternary Sci. Rev., 29, 285–295, 2010.

Yiou, P., Fuhrer, K., Meeker, L. D., Jouzel, J., Johnsen, S., and Mayewski, P. A.: Paleoclimatic variability inferred from the spectral analysis of Greenland and Antarctic ice-core data, J. Geophys. Res., 102, 26441–26454, 1997.